The Exported Chaperone PfHsp70x Is Dispensable for the *Plasmodium falciparum* Intraerythrocytic Life Cycle

David W. Cobb,[a] Anat Florentin,[a,b] Manuel A. Fierro,[a] Michelle Krakowiak,[a] Julie M. Moore,[b,c] (ID) Vasant Muralidharan[a,b]

Department of Cellular Biology, University of Georgia, Athens, Georgia, USA[a]; Center for Tropical and Emerging Global Diseases, University of Georgia, Athens, Georgia, USA[b]; Department of Infectious Diseases, University of Georgia, Athens, Georgia, USA[c]

ABSTRACT Export of parasite proteins into the host erythrocyte is essential for survival of *Plasmodium falciparum* during its asexual life cycle. While several studies described key factors within the parasite that are involved in protein export, the mechanisms employed to traffic exported proteins within the host cell are currently unknown. Members of the Hsp70 family of chaperones, together with their Hsp40 cochaperones, facilitate protein trafficking in other organisms, and are thus likely used by *P. falciparum* in the trafficking of its exported proteins. A large group of Hsp40 proteins is encoded by the parasite and exported to the host cell, but only one Hsp70, *P. falciparum* Hsp70x (PfHsp70x), is exported with them. PfHsp70x is absent in most *Plasmodium* species and is found only in *P. falciparum* and closely related species that infect apes. Herein, we have utilized clustered regularly interspaced short palindromic repeat (CRISPR)/Cas9 genome editing in *P. falciparum* to investigate the essentiality of PfHsp70x. We show that parasitic growth was unaffected by knockdown of PfHsp70x using both the dihydrofolate reductase (DHFR)-based destabilization domain and the *glmS* ribozyme system. Similarly, a complete gene knockout of PfHsp70x did not affect the ability of *P. falciparum* to proceed through its intraerythrocytic life cycle. The effect of PfHsp70x knockdown/knockout on the export of proteins to the host red blood cell (RBC), including the critical virulence factor *P. falciparum* erythrocyte membrane protein 1 (PfEMP1), was tested, and we found that this process was unaffected. These data show that although PfHsp70x is the sole exported Hsp70, it is not essential for the asexual development of *P. falciparum*.

IMPORTANCE Half of the world's population lives at risk for malaria. The intraerythrocytic life cycle of *Plasmodium* spp. is responsible for clinical manifestations of malaria; therefore, knowledge of the parasite's ability to survive within the erythrocyte is needed to combat the deadliest agent of malaria, *P. falciparum*. An outstanding question in the field is how *P. falciparum* undertakes the essential process of trafficking its proteins within the host cell. In most organisms, chaperones such as Hsp70 are employed in protein trafficking. Of the *Plasmodium* species causing human disease, the chaperone PfHsp70x is unique to *P. falciparum*, and it is the only parasite protein of its kind exported to the host (S. Külzer et al., Cell Microbiol 14:1784–1795, 2012). This has placed PfHsp70x as an ideal target to inhibit protein trafficking and kill the parasite. However, we show that PfHsp70x is not required for export of parasite effectors and it is not essential for parasite survival inside the RBC.

KEYWORDS *Plasmodium falciparum*, Hsp70, malaria, protein export

Malaria is a profound killer worldwide. In 2015, 214 million cases of malaria resulted in 438,000 deaths, largely in Africa and Asia (1). Within countries where malaria is endemic, the disease targets the most-vulnerable members of the population, including children less than 5 years old and pregnant women (1). The disease is caused by

infection with eukaryotic parasites from the genus *Plasmodium*, but it is one species—*Plasmodium falciparum*—that is responsible for most of the mortality associated with malaria. The clinical manifestations of malaria range from fever, headache, and muscle pains to severe anemia, coma, and respiratory distress (2). All of these symptoms are direct consequences of asexual replication of the parasite within the human red blood cell (RBC) (3). During this cycle of replication, *P. falciparum* invades the RBC and dramatically transforms its morphology and physiology. Alterations to the RBC include increased permeability, loss of cell deformability, and introduction of virulence-associated knobs at the RBC membrane (4, 5).

Remodeling of the RBC requires export of hundreds of parasite proteins into the host cell, a feat involving protein trafficking through multiple compartments before arriving at their final destinations in the host. The first phase of the journey begins in the parasite endoplasmic reticulum (ER). Many exported proteins contain an N-terminal signal motif termed the host targeting signal or *Plasmodium* export element (PEXEL) (5, 6). A key step in the export of PEXEL-containing proteins is cleavage of the motif by the ER-resident aspartyl protease plasmepsin V (7–9, 45). A subgroup of exported proteins called PEXEL-negative exported proteins (PNEPs) lack the motif, but their N termini are similarly necessary for export (10, 11). Aside from plasmepsin V processing of PEXEL, mechanisms underlying the selection of host-destined proteins for exit from the ER remain unclear. Nonetheless, PEXEL-containing proteins and PNEPs continue their journey through the parasite's secretory pathway and are delivered to the parasitophorous vacuole (PV), a membranous structure within which the parasite resides. Previous studies have shown that proteins cross the parasitophorous vacuole membrane (PVM) through the *Plasmodium* translocon of exported proteins (PTEX) (12–14). Once they are on the other side of the PVM, all classes of proteins need to refold and find their specific subcellular localization, whether it is in the host cytoplasm, host membrane, or parasite-induced structures such as knobs or Maurer's clefts. It is completely unknown how hundreds of proteins, within a short time period, cross through the PTEX, refold to regain structure and function, and find their final destination in the host.

The process of protein export is essential for *P. falciparum* survival in the RBC, as blockage of protein export—whether at the parasite ER or at the PVM—results in death of the parasite. In the ER, overexpression of catalytically dead plasmepsin V (PMV) results in impaired parasite growth, and inhibition of PMV with a PEXEL mimetic impairs protein export and kills parasites during the transition to the trophozoite stage (9, 15, 16). Similarly, *P. falciparum* parasites are sensitive to interference of trafficking across the PVM. Conditional knockdown of PTEX components blocks protein export and kills the parasites (17, 18). As the parasites are susceptible to inhibition of trafficking in the ER and PV, interference in the trafficking process within the host may similarly impair parasite growth. The mechanisms of protein trafficking inside the host cell remain unknown, but identification of essential components of this process will provide valuable targets for drug discovery programs.

Molecular chaperones are likely candidates in the search for key export and trafficking components. Indeed, *P. falciparum* Hsp101 (PfHsp101) is an essential component of PTEX, and its inhibition results in accumulation of exported proteins within the PV (17). Furthermore, several parasite Hsp40s are exported to the RBC, but their function there is unknown (19). In other organisms, Hsp40s serve as cochaperones for Hsp70s, but in contrast to the large number of exported Hsp40s, *P. falciparum* Hsp70x (PfHsp70x) (PF3D7_0831700) is the only parasite-encoded Hsp70 that is exported to the host cell (20, 21). This chaperone is found only in *P. falciparum* and closely related species that cause malaria in apes such as *Plasmodium reichenowi*, but not in other *Plasmodium* species that infect humans, such as *P. vivax* or *P. knowlesi* (20). Within the *P. falciparum*-infected RBC, PfHsp70x is localized to the PV and the host, where it associates with PfHsp40s in mobile structures termed J-dots (20). Given its status as the sole exported Hsp70, we hypothesized that PfHsp70x is central to protein trafficking in the host cell, and thus essential to parasite viability. Indeed, studies focused on PTEX

interactions have found PfHsp70x associated with the translocon, and it has been shown to colocalize with the critical virulence protein PfEMP1 during its trafficking (20, 22, 23).

In this study, we took advantage of various genetic techniques to show that PfHsp70x is nonessential for protein export and parasite growth. We have used the dihydrofolate reductase (DHFR)-based destabilizing domain (DDD) that has previously been used to inhibit chaperone function (17, 24). In addition, we have used the *glmS* ribozyme system that inhibits translation via mRNA degradation (25). Mutants for both knock-down methods were successfully generated, but knockdown had no impact on parasite growth or protein export, including no discernible difference in the export of PfEMP1. To confirm that the lack of a phenotype was not due to incomplete knockdown, we used clustered regularly interspaced short palindromic repeat (CRISPR)/Cas9 technol-ogy to generate a complete knockout of the PfHsp70x gene and found no defects in parasite proliferation or export. Our data demonstrate that PfHsp70x is not required for protein export to the host RBC and not essential for the intraerythrocytic life cycle of *P. falciparum*.

RESULTS

Conditional mutants of PfHsp70x. Previous work has shown that the DHFR-based destabilization domain (DDD) fusions can lead to the inhibition of protein-protein interactions (17, 24) or degradation of the DDD-tagged proteins (26–28). In the pres-ence of the stabilizing ligand trimethoprim (TMP), the DDD is folded, and the chaper-one functions normally. However, upon TMP removal, the DDD is unfolded and binds to its attached chaperone intramolecularly, thereby blocking interactions with the chaperone's client proteins and inhibiting normal chaperone function (see Fig. S1A in the supplemental material). Relying on single-crossover homologous recombination, the *pfhsp70x* gene was modified with a triple-hemagglutinin (triple-HA) tag and the DDD, and integration at the *pfhsp70x* locus was confirmed via Southern blot analysis (Fig. S1A and B). Consistent with the autoinhibitory model of chaperone-DDD action, Western blot analysis of parasite lysates following TMP removal showed that PfHsp70x protein levels remain consistent over time (Fig. S1C). Isolation of the host cell cytoplasm using saponin lysis revealed that PfHsp70x-DDD is exported to the host cell (Fig. S1C). Moreover, the persistence of PfHsp70x in the supernatant following TMP removal indicated that PfHsp70x is exported to the host cell even in its putative inhibited form. To assess the role of PfHsp70x in parasite proliferation, we removed TMP and measured asexual growth over several days and at least two replication cycles. We found that the absence of TMP had no effect on parasite proliferation (Fig. S2A). It was previously reported that PfHsp70x, together with several other exported chaperones, localizes to specific punctate structures in the host cell termed J-dots. To test the effect of DDD-based inhibition on PfHsp70x localization, we performed immunofluorescence assays and found that PfHsp70x-DDD is trafficked to the expected punctate structures within the host cell, regardless of the presence of TMP (Fig. S2B). These data suggest that unlike other chaperones, PfHsp70x activity was unaffected by the DDD fusion or that inhibition of PfHsp70x using the DDD system does not affect the asexual life cycle of the parasite. We therefore utilized alternative methods to reduce PfHsp70x protein levels in the parasite.

Next, we sought to conditionally knock down PfHsp70x at the mRNA level using the *glmS* ribozyme (25). In this system, the *glmS* ribozyme sequence is inserted into the 3′ end of the genomic locus of a gene and is transcribed with the gene as one mRNA. Addition of the small molecule glucosamine (GlcN) activates the *glmS* ribozyme, which cleaves itself from the mRNA, disconnecting the transcript from its poly(A) tail and leading to its degradation (Fig. 1A). Using CRISPR/Cas9 genome engineering, we appended a triple-HA tag to the C terminus of PfHsp70x, followed by the *glmS* ribozyme to make the PfHsp70x-*glmS* protein (Fig. 1A) (29). A second cell line was generated in which the *pfhsp70x* locus was tagged with a mutant version of the ribozyme—termed *M9*—which is unresponsive to GlcN and serves as a control during
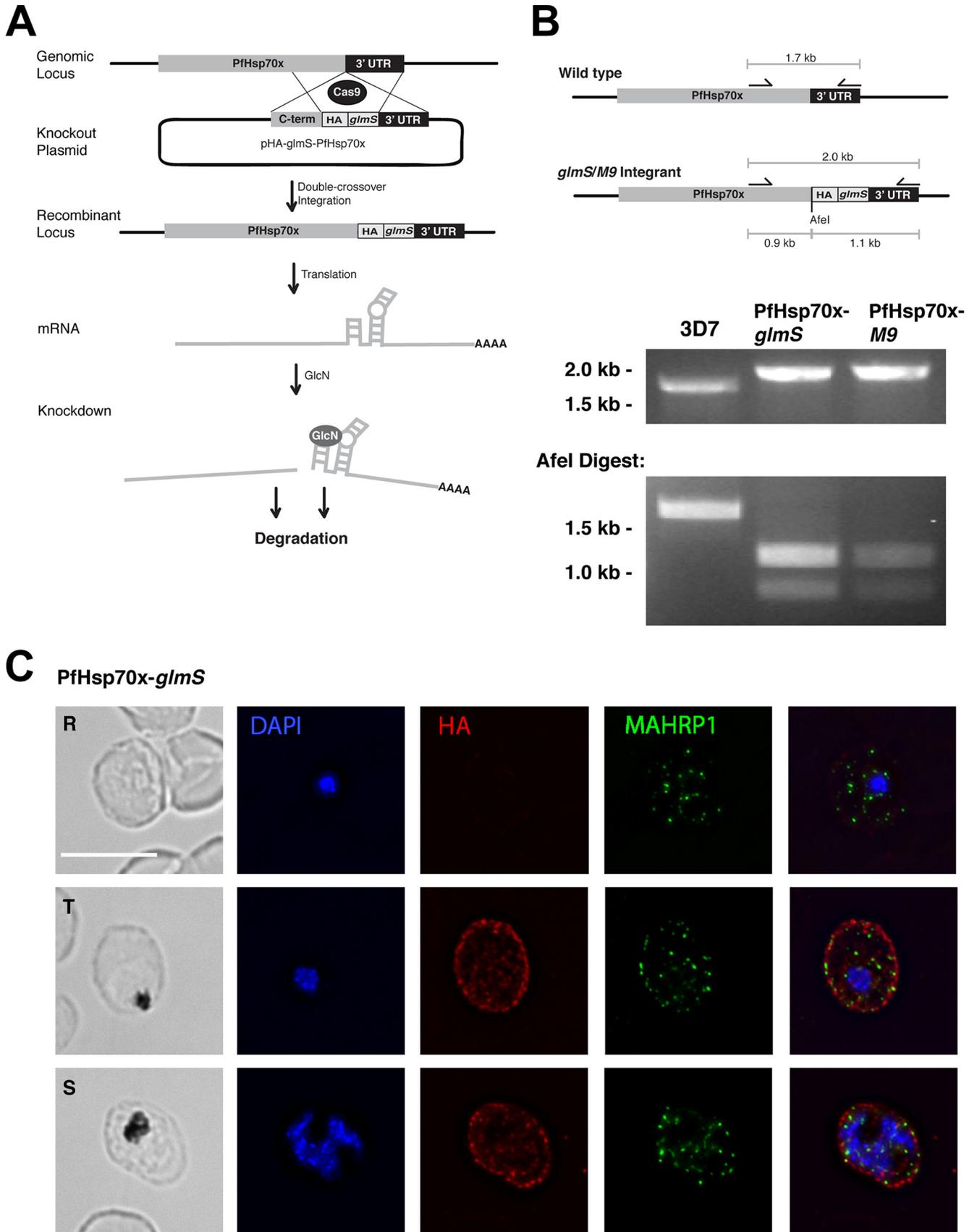
FIG 1 CRISPR/Cas9-mediated integration of HA-glmS/M9 at the PfHsp70x locus. (A) Diagram showing integration of the HA-ribozyme sequence and GlcN-induced degradation of mRNA. Cas9 introduces a double-stranded break at the beginning of the 3′ UTR of the *pfhsp70x* locus. The repair plasmid
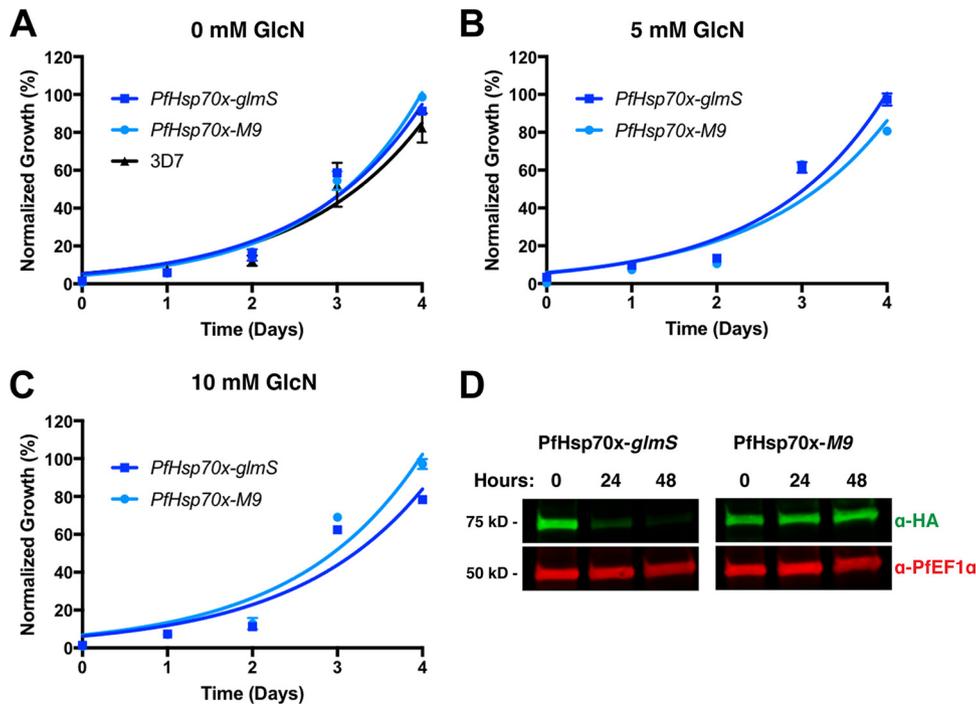
FIG 2 GlcN-induced knockdown of PfHsp70x does not affect intraerythrocytic growth. (A) PfHsp70x-*glmS*, PfHsp70x-*M9*, and 3D7 (parental) cell lines were seeded at equal parasitemia in triplicate and grown in normal culturing medium. Parasitemia was measured every 24 h using flow cytometry. Data are fit to an exponential growth equation and are represented as means ± standard errors of the means (SEM) (error bars) ($n = 3$). (B and C) PfHsp70x-*glmS* and PfHsp70x-*M9* parasites were seeded at equal parasitemia in triplicate. Cultures were grown in the presence of either 5 mM or 10 mM GlcN. Parasitemia was measured every 24 h using flow cytometry. Data are fit to an exponential growth equation and are represented as means ± SEM ($n = 3$). (D) PfHsp70x-*glmS* and PfHsp70x-*M9* parasites were grown in the presence of 7.5 mM GlcN. Schizont-stage parasites were purified on a Percoll gradient every 24 h, and whole-parasite lysates were used for Western blot analysis. The membrane was probed with anti-HA (α-HA) and anti-PfEF1α (loading control) antibodies. The positions of molecular mass markers (in kilodaltons) are indicated to the left of the blot.

GlcN treatment (25). Following transfection and drug selection, PfHsp70x-*glmS* and PfHsp70x-*M9* clones were isolated via limiting dilutions. PCR analysis revealed the correct integration of the tag and ribozyme into the *pfhsp70x* gene in all clonal parasite lines (Fig. 1B). Additionally, immunofluorescence assays confirmed that the PfHsp70x-*glmS* protein is exported to the host cytoplasm, where it is found, as before, in punctate structures that are distinct from Maurer's clefts, suggestive of J-dot localization (Fig. 1C).

Next, we tested the effects of reducing PfHsp70x levels on intraerythrocytic growth. To ensure that insertion of the ribozyme itself does not interfere with normal asexual growth, the PfHsp70x-*glmS* and PfHsp70x-*M9* cell lines and the parental line (3D7) were grown in the absence of GlcN. Indeed, we found that in the absence of GlcN, growth of both the *glmS* and *M9* cell lines was comparable to the growth of 3D7 (Fig. 2A). Next, the PfHsp70x-*glmS* and PfHsp70x-*M9* cell lines were cultured with GlcN, and parasitemia was measured via flow cytometry. The growth of PfHsp70x-*glmS* and PfHsp70x-*M9* cell lines was unaffected by treatment with 5 mM and 10 mM GlcN

FIG 1 Legend (Continued)

provides homology regions for double-crossover homologous recombination, introducing a triple-hemagglutinin (HA) tag and the ribozyme sequence. Following translation and addition of glucosamine (GlcN), the PfHsp70x-*glmS* mRNA is cleaved by the ribozyme and is subject to degradation. C-term, C terminus. (B) PCR test confirming integration at the PfHsp70x locus. DNA was purified from transfected, cloned parasites, and primers were used to amplify the region between the C terminus and the 3′ UTR of *pfhsp70x*. The PCR products were digested with AfeI, further confirming integration. (C) IFA showing export of HA-tagged PfHsp70x. Asynchronous PfHsp70x-*glmS* parasites were fixed with acetone and stained with specific antibodies. From left to right, the images are phase-contrast micrographs of parasites, parasites stained with DAPI (parasite nucleus) (blue), parasites stained with anti-HA antibody (red), parasites stained with anti-MAHRP1 antibody (green), and fluorescence merge images of the parasites. Abbreviations: R, rings; T, trophozoites; S, schizonts. Bar, 5 μm.
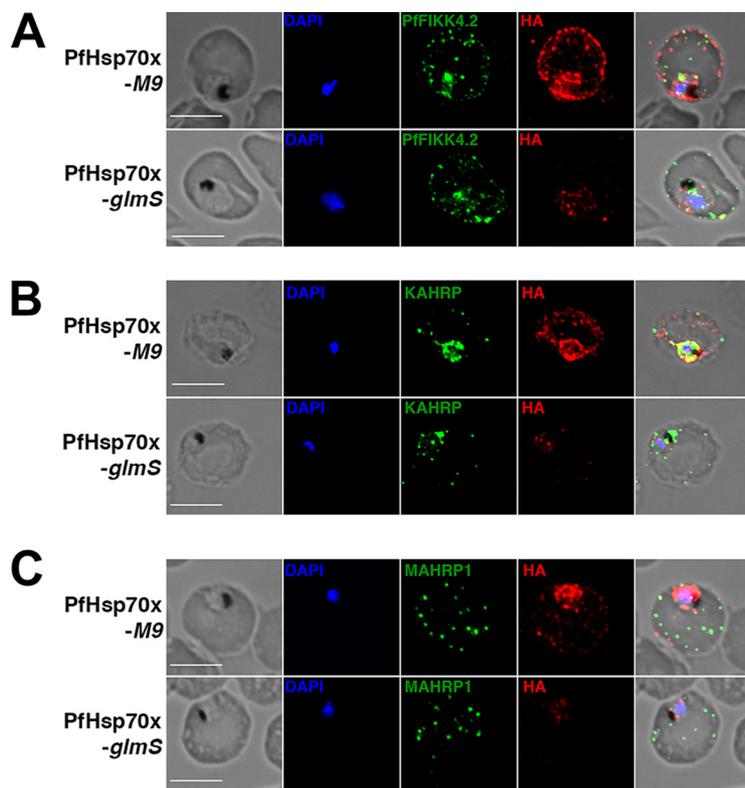
FIG 3 PfHsp70x knockdown does not inhibit export of virulence-associated proteins. Asynchronous PfHsp70x-*M9* and PfHsp70x-*glmS* parasites were fixed with acetone (PfFIKK4.2 and MAHRP1) or paraformaldehyde (KAHRP) and stained with antibodies against PfFIKK4.2 (A), KAHRP (B), or MAHRP1 (C). DAPI was used to mark parasite cell nucleus. From left to right, the images are phase-contrast micrographs of parasites, parasites stained with DAPI (blue), parasites stained with antibody against the exported protein (green), parasites stained with anti-HA antibody (red), and fluorescence and phase-contrast merge images of the parasites. Representative images are shown. Bars, 5 μm.

(Fig. 2B and C). To confirm that the level of PfHsp70x protein is reduced in response to GlcN, schizont-stage parasites from the *glmS* and *M9* cell lines were purified with Percoll, and whole-parasite lysates were used for Western blotting. Using anti-HA antibody, we found that treatment with GlcN reduced protein levels in the PfHsp70x-*glmS* cell line but did not affect protein levels in the PfHsp70x-*M9* cell line (Fig. 2D). Together, these data show that we can efficiently reduce PfHsp70x levels using the *glmS* ribozyme, but this has no effect on the asexual growth of the parasite within the RBC.

Protein export is unimpaired in PfHsp70x knockdown parasites. Although parasite growth was unaffected by PfHsp70x knockdown, we reasoned that it could nonetheless play a role in export of proteins to the host cell. In particular, we hypothesized that PfHsp70x is needed for the export of proteins known to mediate virulence of *P. falciparum* infection, as trafficking defects of these proteins would not manifest as arrest of the asexual life cycle (19). Using immunofluorescence, we examined localization of specific virulence-associated proteins in PfHsp70x-*M9* and PfHsp70x-*glmS* parasites after 72 h of growth in GlcN-supplemented medium. First, the localization of the PEXEL-containing PfFIKK4.2, an exported kinase associated with knob formation and infected RBC rigidity, is unchanged in control versus PfHsp70x knockdown parasites (Fig. 3A) (30). Next, we examined the localization of the PEXEL-containing protein KAHRP (knob-associated histidine-rich protein), which is essential for the formation of knobs on the surfaces of infected RBCs (31). Export of this protein was not inhibited in PfHsp70x knockdown parasites (Fig. 3B). Finally, we determined the localization of the PNEP MAHRP1 (Maurer's cleft histidine-rich protein 1), which has
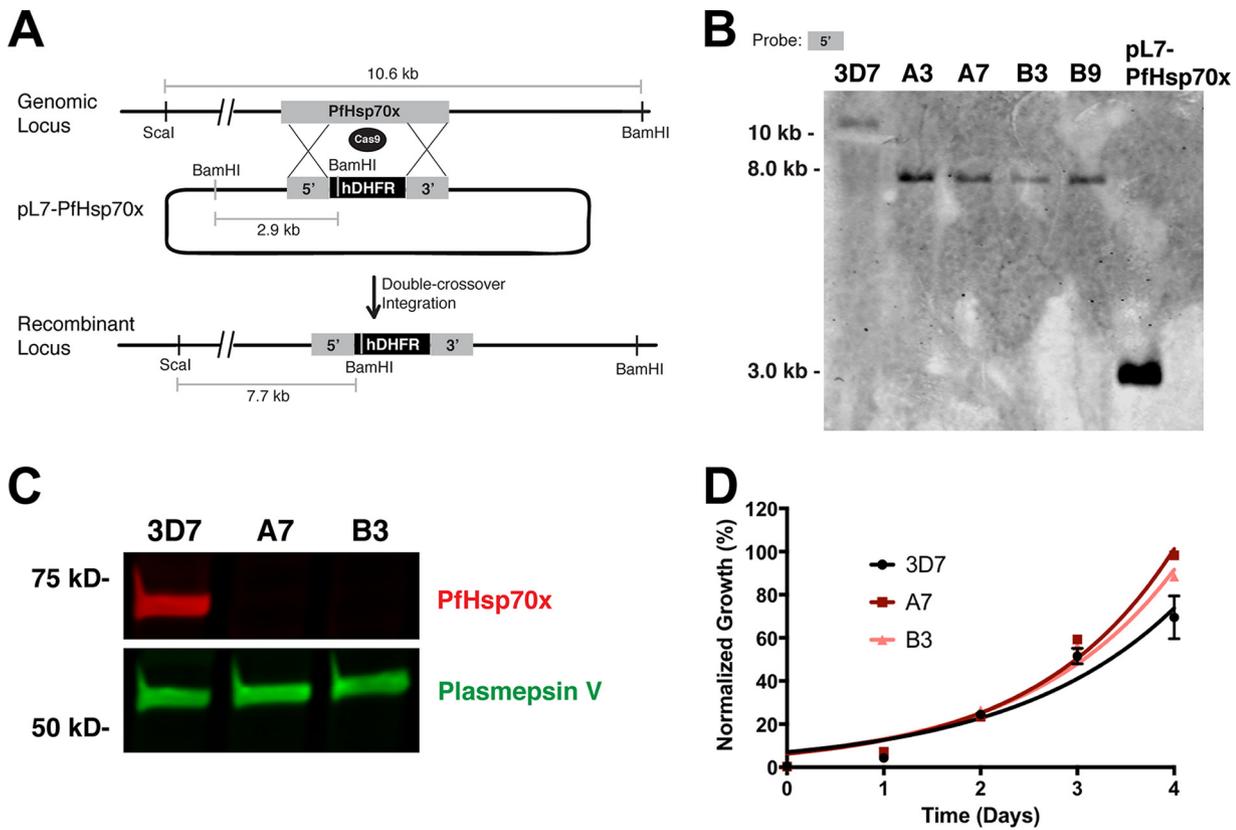
FIG 4 Knockout of *pfhsp70x* does not affect intraerythrocytic growth. (A) Schematic representation showing interruption of the PfHsp70x ORF with the *hDHFR* cassette. The Cas9-mediated double-stranded break in the *pfhsp70x* ORF is repaired using homology regions on the template plasmid while inserting an *hDHFR* cassette into the locus. (B) Southern blot analysis confirming knockout of PfHsp70x. Genomic DNA from independent knockout clones (A3, A7, B3, and B9) was isolated and digested with BamHI and ScaI. The membrane was hybridized with a biotin-labeled probe complementary to the first 800 bp of the *pfhsp70x* ORF. (C) Western blot analysis demonstrating loss of PfHsp70x protein expression in independent knockout clones. Schizont-stage parasites were purified on a Percoll gradient, and whole-cell lysate was used for analysis. The membrane was probed with antibody raised against PfHsp70x and antibody against plasmepsin V as a loading control. (D) Parental lines and independent PfHsp70x-KO clones (A7 and B3) were seeded at equal parasitemia in triplicate. Parasitemia was measured every 24 h using flow cytometry. Data are fit to an exponential growth equation and are represented as means ± SEM ($n = 3$).

been implicated in the presentation of antigenically variant proteins, including PfEMP1, at the RBC surface, and we found that its export is not impaired by the knockdown of PfHsp70x (Fig. 3C) (32). As demonstrated by HA staining of Western blots and indirect immunofluorescence assay (IFA) (Fig. 2D and Fig. 3), PfHsp70x is reduced, but not completely ablated, using the *glmS* ribozyme. We reasoned that the reduced level of PfHsp70x that is produced during GlcN treatment could be sufficient for parasite survival, and therefore endeavored next to knock out *pfhsp70x*.

Knockout of *pfhsp70x* does not affect parasite growth. We utilized two different conditional knockdown systems to modify the PfHsp70x locus, but these approaches were insufficient to produce a growth defect in the parasites. Therefore, we sought to definitively test the essentiality of PfHsp70x via complete genomic knockout (KO). To this end, we employed CRISPR/Cas9 to interrupt the PfHsp70x open reading frame (ORF) by inserting a human dihydrofolate reductase (*hdhfr*) drug resistance cassette (Fig. 4A). Following transfection and selection with WR99210, PfHsp70x-KO parasites were cloned via limiting dilutions. Southern blot analysis of genomic DNA isolated from the parental line and independent clones showed that the *hdhfr* cassette was inserted into the *pfhsp70x* gene via homology-directed repair (Fig. 4B). To verify that the null mutants do not express PfHsp70x, schizont-stage parasites from two independent knockout clones and the parental line were purified on a Percoll gradient, and whole-parasite lysates were used for Western blotting. Probing with anti-PfHsp70x shows that the knockout clones do not express PfHsp70x (Fig. 4C). Intraerythrocytic growth of the
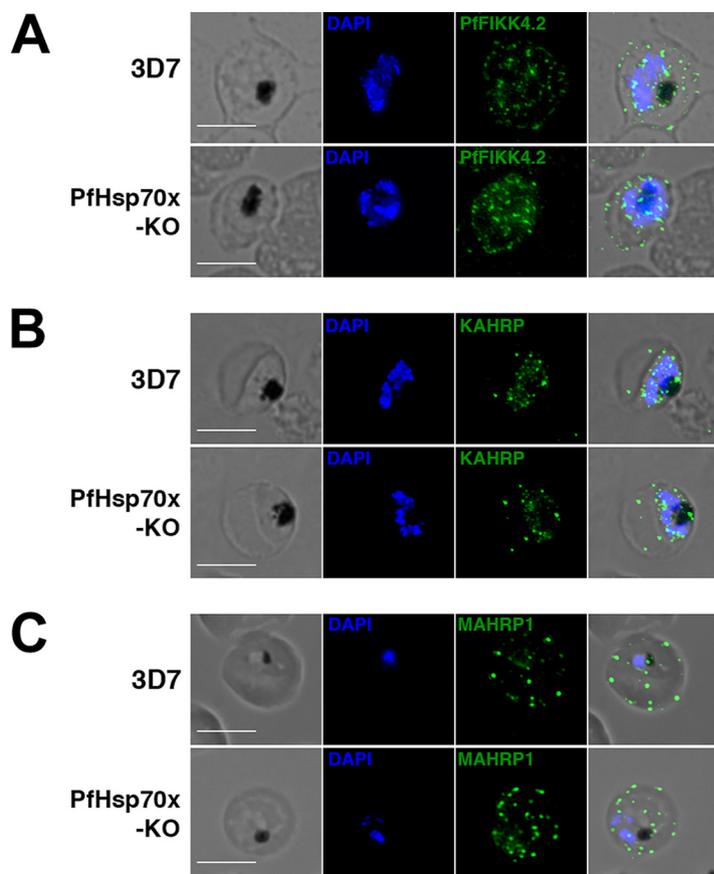
FIG 5 PfHsp70x knockout does not inhibit export of virulence-associated proteins. Asynchronous 3D7 and PfHsp70x-KO parasites were fixed with acetone (PfFIKK4.2 and MAHRP1) or paraformaldehyde (KAHRP) and stained with antibodies against PfFIKK4.2 (A), KAHRP (B), or MAHRP1 (C). DAPI was used to mark parasite cell nucleus. From left to right, the images are phase-contrast micrographs of the parasites, parasites stained with DAPI (blue), parasites stained with antibody against exported protein (green), and fluorescence and phase-contrast merge. Representative images are shown. Bars, 5 μm.

PfHsp70x-KO clones was monitored over two replication cycles. In agreement with the lack of any growth phenotype in the conditional knockdown parasite lines, the PfHsp70x-KO parasites displayed wild-type level of proliferation in erythrocytes (Fig. 4D). Finally, we measured the susceptibility of PfHsp70x-KO clones to heat shock stress by monitoring their growth after a heat shock (Fig. S3). These data show that the PfHsp70x-KO parasites are able to deal with heat shock just as well as the wild-type parasites (Fig. S3). The normal growth in the complete absence of PfHsp70x expression conclusively demonstrates that PfHsp70x activity is not essential for the asexual growth of the parasite within the RBC.

Protein export is unimpaired in PfHsp70x-KO parasites. Using PfHsp70x-KO parasites, we next tested the hypothesis that the chaperone is required for export of virulence-associated proteins. Using immunofluorescence, we examined the export of the same proteins assayed with PfHsp70x-*glmS* parasites: PfFIKK4.2, KAHRP, and MAHRP1 (30–32). Consistent with our observations using PfHsp70x-*glmS*, *pfhsp70x* knockout did not interrupt export of these proteins (Fig. 5). These data show that the loss of PfHsp70x does not impede the parasite's ability to export virulence-associated proteins to the host cell.

Export of antigenic proteins to the host RBC is unaffected in PfHsp70x mutants. PfHsp70x was shown to interact with the antigenically variant protein PfEMP1, and recent data that identified proteins that interact with PfEMP1 confirm these results (20). Therefore, we wanted to test how the export of PfEMP1 is affected in our mutants.
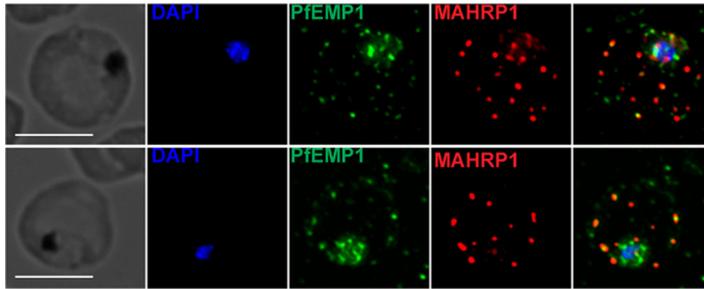
FIG 6 PfHsp70x knockout does not inhibit export of PfEMP1 to the host cell. Asynchronous 3D7 and PfHsp70x-KO parasites were fixed with acetone and stained with antibodies against the ATS domain of PfEMP1 and MAHRP1. DAPI was used to stain parasite cell nucleus. The images from left to right are phase, DAPI (blue), PfEMP1 (green), MAHRP1 (red), and fluorescence merge. Representative images are shown.

Utilizing immunofluorescence microscopy, we determined the localization of PfEMP1 in 3D7 and PfHsp70x-KO parasites (Fig. 6). Our data show that knockout of PfHsp70x does not prevent export of PfEMP1 to the host cell (Fig. 6). Next, we observed the export of PfEMP1 in our PfHsp70x conditional mutants. Our data show that PfEMP1 is exported equally well in both PfHsp70x-*M9* and PfHsp70x-*glmS* parasites under knockdown conditions (Fig. 7). We quantified the amount of PfHsp70x-HA, as well as the amount of exported PfEMP1, in these mutants and found no difference in regard to PfEMP1, despite achieving significant reduction of PfHsp70x in the *glmS* parasite line (Fig. 7A and B). Because MAHRP1 has been implicated in the trafficking of PfEMP1, we also quantified the export of MAHRP1 in the PfHsp70x conditional mutants, and we found that knockdown of PfHsp70x does not affect MAHRP1 export (Fig. 7C).

Next, we sought to investigate whether there were any differences in the mutants in the export of antigenic parasite proteins that generate an immune response. We obtained pooled human sera collected from a region where malaria is endemic (Kenya) as well as a region where it is not endemic (United States) (33). Uninfected RBCs, 3D7 parasites, and PfHsp70x-KO parasites were labeled with these sera and observed via flow cytometry (Fig. 8). 3D7 and PfHsp70x-KO schizonts were synchronized and grown to the schizont stage, and cultures were brought to identical parasitemia prior to labeling with sera. Our data show that both 3D7 and PfHsp70x-KO parasites are labeled equally well by human sera collected from regions where malaria is endemic but not by sera obtained from regions where malaria is not endemic, suggesting that the export of antigenic parasite proteins to the host RBC is unaffected by the loss of PfHsp70x (Fig. 8).

DISCUSSION

While this work was under review, another study was published showing that knockout of PfHsp70x did not affect parasite growth (34). In agreement with these data, our data also demonstrate that PfHsp70x is not required for intraerythrocytic growth, even though PfHsp70x is the only parasite-encoded Hsp70 that is exported to the RBC (Fig. 2A, B, and C and Fig. 4D; also see Fig. S2A and Fig. S3D in the supplemental material). Using two different genetic approaches, we demonstrate that the export of several parasite effectors are unaffected by the loss of PfHsp70x (Fig. 3 and Fig. 5 to 8). In the case of PfEMP1, the newly published work suggests that knockout of PfHsp70x led to delays in its export and minor loss in cytoadherence, suggesting a role for PfHsp70x in parasite virulence (34). In this case, the data show that PfHsp70x knockout parasites overexpress some exported proteins (34). This suggests that there may be compensatory mechanisms that are activated when PfHsp70x is knocked out and therefore lead to minor, if any, changes in the export of parasite virulence factors (34). However, this interpretation is clouded by the lack of a conditional mutant for PfHsp70x, which cannot compensate for the loss of PfHsp70x. The data described in this study show that in both PfHsp70-KO and PfHsp70x-*glmS* mutants, export of parasite
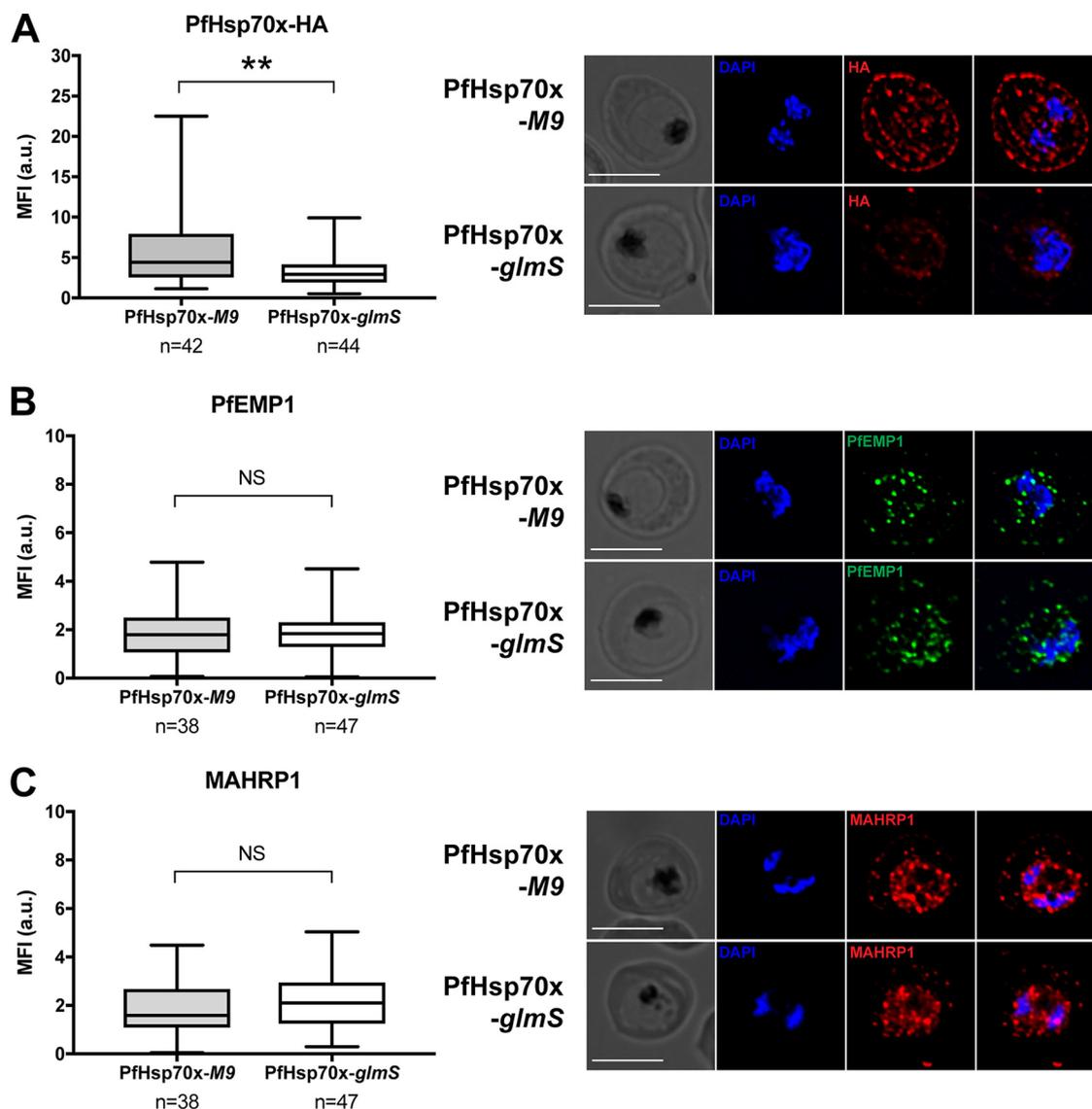
FIG 7 Knockdown of PfHsp70x does not inhibit export of PfEMP1 to the host cell. (A to C) PfHsp70x-*M9* and PfHsp70x-*glmS* parasites were fixed with acetone and stained with antibodies against HA, PfEMP1, or MAHRP1. DAPI was used to mark parasite cell nucleus. (Right) From left to right, the images are phase-contrast micrographs of parasites, parasites stained with DAPI, parasites stained with anti-HA antibody or antibody against exported protein, and fluorescence merge image. Representative images are shown. Bars, 5 μm. (Left) The mean fluorescence intensity (MFI) for each protein was calculated for individual cells and shown as box-and-whisker plots, with whiskers representing the maximum and minimum MFI. For HA, the MFI was calculated for the entire infected RBC. For PfEMP1 and MAHRP1, MFI was calculated for the exported fraction only. Significance was determined using an unpaired *t* test (**, $P \leq 0.01$; NS, not significant).

virulence factors is not affected (Fig. 3 and Fig. 5 to 8). We specifically tested the export of the antigenically variant protein, PfEMP1, which is responsible for cytoadherence, and observed that the export of PfEMP1 was unaffected in either the knockout or conditional mutants of PfHsp70x (Fig. 6 to 8). Therefore, our data suggest a slightly different, though not mutually exclusive, model than the one proposed by Charnaud et al. (34). PfHsp70x is not the only Hsp70 found in infected RBCs. Several human chaperones, including Hsp70, are present in the erythrocyte cytoplasm (35). Thus, the role played by PfHsp70x in the parasite's biology could be redundant with the human Hsp70 that is already present in the host cell. In fact, infection with *P. falciparum* affects the normal localization of the human Hsp70, as the protein is soluble in nonparasitized RBCs but is found in detergent-resistant fractions following infection (36). Another paper published while this work was under review identified several interacting part-
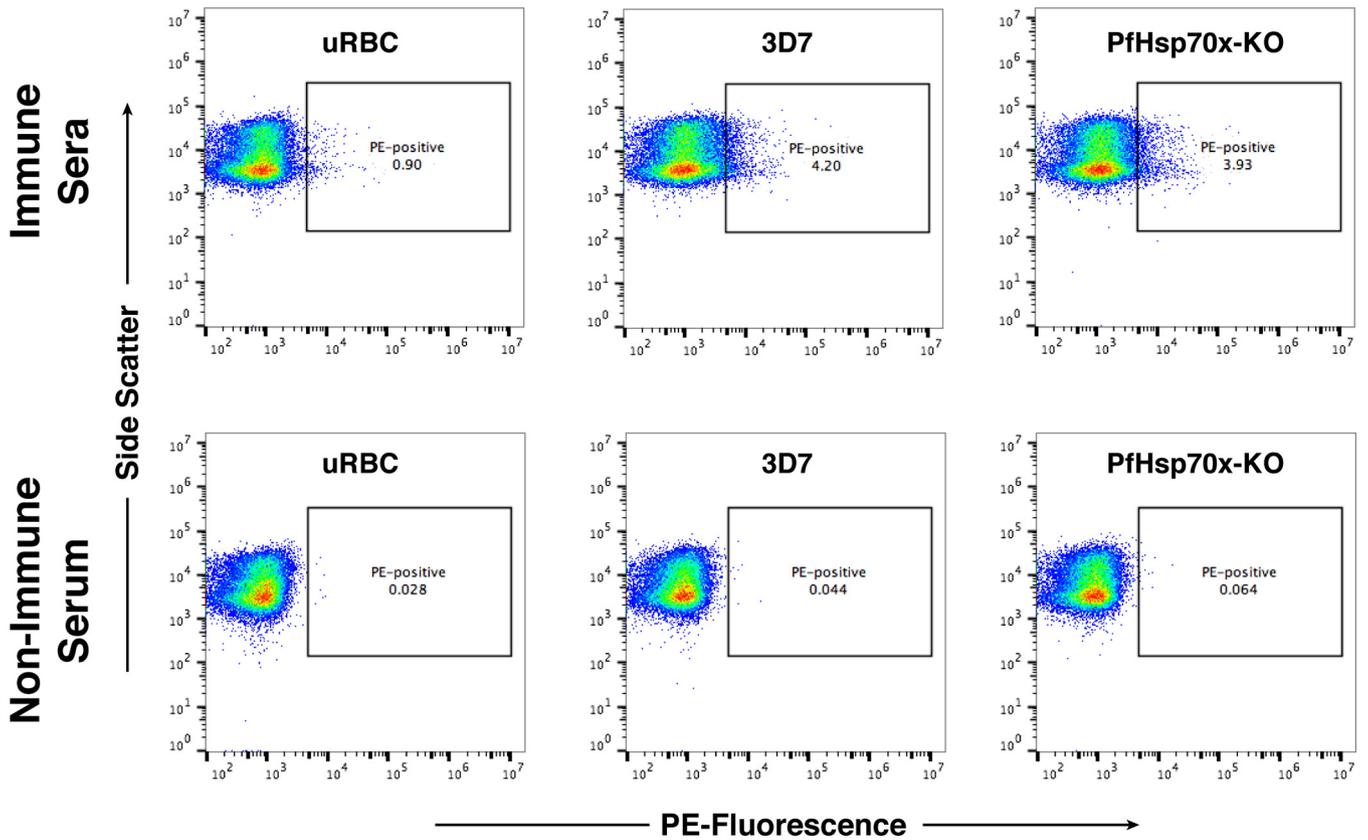
FIG 8 Human immune sera recognizes 3D7 and PfHsp70x-KO parasites. Synchronized 3D7 and PfHsp70x-KO parasites were incubated with either pooled human sera from Kenya where malaria is endemic (top panels) or pooled nonimmune human serum from the United States (bottom panels). Recognition by the serum was determined using a PE-conjugated anti-human IgG antibody and flow cytometry. Uninfected red blood cells (uRBC) were also assayed. Side scatter is shown on the y axes, and PE fluorescence is shown on the x axes.

ners of PfEMP1 using thorough proteomic and genetic data (37). They identified several human chaperones, specifically from the TRiC chaperonin complex, that interact with PfEMP1. Together with our data, this suggests a model wherein PfEMP1 export is aided both by PfHsp70x and by human chaperones present in the host RBCs. This further suggests that loss of either one of them may not be enough to derail the export of parasite virulence proteins to the host RBC. The methods used here to investigate the function of PfHsp70x, knockdown and complete genomic knockout, are more challenging to use for human chaperones such as Hsp70 or the TRiC chaperonin complex. The mature RBC cannot be genetically manipulated, and knockdown of human Hsp70 in hematopoietic stem cells abrogates RBC formation (38). Our data demonstrate that pooled human sera collected from regions where malaria is endemic are unable to differentiate between wild-type and PfHsp70x-KO parasites, raising the possibility that PfHsp70x may not be required in human infections (Fig. 8). However, further detailed analysis of the *pfhsp70x* locus in strains isolated from the field or testing its role in other stages of the parasite life cycle may be informative about the essentiality of PfHsp70x in human infections. Overall, our data demonstrate that PfHsp70x is not required for export of *P. falciparum* effector proteins to the host and is dispensable for asexual growth within human RBCs and suggest a model where both human chaperones and parasite chaperones act in a redundant manner to ensure export of parasite virulence factors to the host RBCs.

MATERIALS AND METHODS

Plasmid construction. Genomic DNA was isolated from *P. falciparum* using the QIAamp DNA blood kit (Qiagen). Constructs utilized in this study were confirmed by sequencing. PCR products were inserted into the respective plasmids using the In-Fusion cloning system (Clontech) or using the sequence- and ligation-independent cloning (SLIC) method. Briefly, insert and cut vector were mixed with a T4 DNA

polymerase and incubated for 2.5 min at room temperature, followed by 10-min incubation on ice, and then transformed into bacteria. For generation of plasmid PfHsp70x-HADB, a 1-kb homologous sequence from the 3′ end of the *pfhsp70x* gene (not including the stop codon) was amplified by PCR using primers 5′ CACTATAGAACTCGAGGTGAAAAAGCTAAACGTGTATTATCATCATCCGCACAAGC 3′ and 5′ CGTATGGGT ACCTAGGATTTACTTCTTCAACGGTTGGTCCATTATTTTGTGC 3′ and inserted into pHADB (16) using restriction sites XhoI and AvrII (New England Biolabs).

For the generation of the *glmS* conditional mutants, three plasmids were used. (i) pUF1-Cas9 (from J. J. Lopez-Rubio) was used to drive cas9 expression (29). (ii) pMK-U6 was used to drive expression of the RNA guide. For this purpose, pL6 plasmid (from J. J. Lopez-Rubio [29]) was digested with NotI and NcoI (New England Biolabs), and the fragment that contained the U6 RNA expression cassette was blunted and religated to form the pMK-U6 plasmid. The guide RNA, oligonucleotides 5′ TAAGTATATAATATTTG CATTATTGTTGTATATTTGTTTTAGAGCTAGAA 3′ and 5′ TTCTAGCTCTAAAACAAATATACAACAATAATGCAA ATATTATATACTTA 3′ were annealed and cloned into the RNA module in MK-U6 as previously described (29). Briefly, pMK-U6 was digested with BtgZI (New England Biolabs), and annealed oligonucleotides were inserted using In-Fusion HD Cloning kit (Clontech). (iii) pHA-glmS and pHA-M9 were used as donor DNA templates consisting of two homology regions flanking the hemagglutinin (HA) tag and the *glmS* (or the *M9*) sequences. To generate the pHA-glmS and pHA-M9 plasmids, primers 5′ GAGCTCGCTAGCAAGCTT GCCGGCAAGATCATGTGATTTCTCTTTGTTCAAGGAGTC 3′ and 5′ TCCGCGGAGCGCTACTAGTTACCCATAC GATGTTCCAGATTACGCTTACCCATACGATGTTCCAGATTACGCTTACCCATACGATGTTCCAGATTACGCTTAAAT GTCCAGACCTGCAGTAATTATCCCGCCCGAACTAAGCGC 3′ were used to amplify the *glmS* and *M9* sequences from pGFP-glmS and pGFP-M9, respectively (from P. Shaw [25]). PCR constructs were then inserted into a TOPO cloning vector (Thermo Fisher). To allow efficient genomic integration of the pHA-glmS and pHA-M9 donor plasmids, 800-bp sequences were used for each homology region. The C terminus of the *pfhsp70x* coding region was PCR amplified from genomic DNA using primers 5′ AATTCGCCCTTCCGCGGGCTGTACAA GCAGCCATCTTATCAGGTGATCAATCATC 3′ and 5′ ATCGTATGGGTAAGCGCTATTTACTTCTTCAACGGTTGGTCC ATTATTTTGTGCTTC 3′ and inserted into pHA-glmS and pHA-M9 using restriction sites SacII and AfeI (New England Biolabs). The 3′ untranslated region (3′ UTR) of *pfhsp70x* was PCR amplified from genomic DNA using primers 5′ ATGATCTTGCCGGCAAGCTTACGAAAATATACAACAATAATGCATAAAATAATAATAATT 3′ and 5′ CC TTGAGCTCGCTAGCGCAATATAAATGGATTATTCCTTTTGTATATAATTTAAAATAAG 3′ and inserted into pHA-glmS and pHA-M9 (already containing the C-terminal homology region) using restriction sites HindIII and NheI (New England Biolabs).

For the generation of *pfhsp70x-ko* parasites, two plasmids were used: (i) a cas9-expressing plasmid (as described above), and (ii) pL7-PfHsp70x plasmid that is derived from the pL6 plasmid (from J. J. Lopez-Rubio [29]). pL7-PfHsp70x contained the guide RNA and 800-bp homology regions flanking an *hdhfr* gene that confers resistance to WR99210. The N terminus of the *pfhsp70x* gene was amplified via PCR from genomic DNA using primers 5′ cggggaggactagtATGAAGACAAAAATTTGTAGTTATATTCATTAT ATTG 3′ and 5′ acaaaatgcttaagGGAAACATCTTTACCTCCATTTTTTTTTTTAAAATCTTGTAC 3′ (lowercase nucleotides are not part of the *pfhsp70x* gene but are part of the plasmid used for sequence and ligation independent cloning [SLIC]) and inserted into pL6 using restriction sites AflII and SpeI (New England Biolabs). The C terminus of the *pfhsp70x* gene was PCR amplified from genomic DNA using primers 5′ taaatctagaattcTGATCAATCATCAGCTGTCAAAGACTTATTATTATTAGATG 3′ and 5′ ttaccgttccatggTTAATTT ACTTCTTCAACGGTTGGTCCATTATTTTGTGCTTC 3′ and inserted into pL6 (already containing the C-terminal homology region) using restriction sites NcoI and EcoRI (New England Biolabs). In order to insert the guide DNA sequence, oligonucleotides 5′ TAAGTATATAATATTGTACAAGCAGCCATCTTATCGTTTTAG AGCTAGAA 3′ and 5′ TTCTAGCTCTAAAACGATAAGATGGCTGCTTGTACAATATTATATACTTA 3′ were annealed and cloned into pL6 as previously described (29). Briefly, pL6 was digested with BtgZI (New England Biolabs), and annealed oligonucleotides were inserted using In-Fusion HD cloning kit (Clontech).

Cell culture and transfections. Parasites were cultured in RPMI 1640 medium supplemented with Albumax I (Gibco) and transfected as described earlier (39, 40). For generation of *PfHsp70x-DDD* parasites, PfHsp70x-HADB was transfected in duplicate into 3D7-derived parental strain PM1KO (KO stands for knockout) which contains a human dihydrofolate reductase (*hDHFR*) expression cassette conferring resistance to trimethoprim (TMP) (41). Selection and drug cycling were performed as described previously (24) in the presence of 10 μM TMP (Sigma). Integration was detected after three rounds of drug cycling with blasticidin (Sigma).

For generation of PfHsp70x-*glmS* and PfHsp70x-*M9* parasites, a mix of three plasmids (40 μg of each) was transfected in duplicate into 3D7 parasites. The plasmid mix contained pUF1-Cas9 (from J. J. Lopez-Rubio [29]) which contains the *DHOD* resistance gene, pMK-U6-PfHsp70x, pHA-glmS-PfHsp70x, or pHA-M9-PfHsp70x, which are all marker-free. Drug pressure was applied 48 h posttransfection, using 1 μM (DSM1) (42), selecting only for Cas9 expression. Drug was removed from the culturing medium once the parasites were detected in the culture, usually around 3 weeks posttransfection.

For generation of PfHsp70x-KO parasites, a mix of pUF1-Cas9 (from J. J. Lopez-Rubio [29]) and pL7-PfHsp70x (50 μg of each plasmid) was transfected in duplicate into 3D7 parasites. Drug pressure was applied 48 h posttransfection, using 2.5 nM WR99210 (Sigma), selecting for integration of the drug resistance cassette into the *pfhsp70x* gene.

Growth assays. For asynchronous growth assays of PfHsp70x-DDD lines, parasites were washed twice and incubated without TMP. For asynchronous growth assays of PfHsp70x-*glmS* and PfHsp70x-*M9* parasites, 5 or 10 mM glucosamine (GlcN) (Sigma) was added to the growth medium. Asynchronous growth assays of PfHsp70x-KO parasites were performed in medium containing WR99210. Parasitemia was monitored every 24 h via flow cytometry. For flow cytometry, aliquots of parasite cultures (5 μl) were stained with 1.5 mg/ml acridine orange (Molecular Probes) in phosphate-buffered saline (PBS). The

fluorescence profiles of infected erythrocytes were measured by flow cytometry on a CyAn ADP (Beckman Coulter) or CytoFLEX (Beckman Coulter) instrument and analyzed by FlowJo software (Treestar, Inc.). Whenever required, parasites were subcultured to avoid high parasite density, and relative parasitemia at each time point was back-calculated based on actual parasitemia multiplied by the relevant dilution factors. One hundred percent parasitemia was determined as the highest relative parasitemia and was used to normalize parasite growth. Data were fit to exponential growth equations using Prism (GraphPad Software, Inc.).

Southern blotting. Southern blotting was performed with genomic DNA isolated using the Qiagen Blood and Cell Culture kit. Ten micrograms of DNA was digested overnight with NcoI/XmnI for PfHsp70x-DDD and BamHI/ScaI for PfHsp70x-KO (New England Biolabs). Integrants were screened using biotin-labeled probes against the 3′ end (PfHsp70x-DDD parasites) or 5′ end (PfHsp70x-KO parasites) of the *pfhsp70x* open reading frame (ORF). Southern blotting was performed as described earlier (43). The probe was labeled using biotinylated biotin-16-dUTP (Sigma). The biotinylated probe was detected on blots using IRDye 800CW streptavidin-conjugated dye (LICOR Biosciences) and imaged, processed, and analyzed using the Odyssey infrared imaging system software (LICOR Biosciences).

Western blotting. Western blotting was performed as described previously (26). Briefly, late-stage parasites were isolated on a Percoll gradient (Genesee Scientific). For PfHsp70x-DDD parasites, host red blood cells (RBCs) were permeabilized selectively by treatment with ice-cold 0.04% saponin in PBS for 10 min. Supernatants were collected for detection of exported parasite proteins, and pellets were collected for detection of proteins with the parasite. For PfHsp70x-KO, PfHsp70x-*glmS*, and PfHsp70x-*M9* parasites, whole-parasite lysates, including the host RBCs, were used to detect protein expression and export. The antibodies used in this study were rat anti-HA (3F10; Roche) (diluted 1:3,000), rabbit anti-PfEF1α (from D. Goldberg) (1:2,000), mouse anti-plasmepsin V (from D. Goldberg, 1:400), and rabbit anti-PfHsp70x (from J. Przyborski) (1:1,000). The secondary antibodies that were used are IRDye 680CW goat anti-rabbit IgG and IRDye 800CW goat anti-mouse IgG (LICOR Biosciences) (1:20,000). The Western blot images were processed and analyzed using the Odyssey infrared imaging system software (LICOR Biosciences).

Microscopy and image processing. For detection of HA tags, PfHsp70x, PfFIKK4.2, and MAHRP1, cells were smeared on a slide and fixed with acetone. For KAHRP detection, cells were fixed with paraformaldehyde and glutaraldehyde. PfHsp70x-HA was detected using rat anti-HA antibody (clone 3F10; Roche) (1:100). MAHRP1 was detected using rabbit anti-MAHRP1 (from Hans-Peter Beck) (1:500). PfFIKK4.2 and KAHRP were detected using mouse anti-PfFIKK4.2 (1:1,000) and mouse anti-KAHRP (1:1000 and 1:500, respectively; both antibodies acquired from David Cavanagh and EMRR). PfEMP1 was detected using mouse anti-ATS (1B/98-6H1-1; 1:100; Alan Cowman). Secondary antibodies used were anti-rat antibody conjugated to Alexa Fluor 488 or 594, anti-rabbit antibody conjugated to Alexa Fluor 488, and anti-mouse antibody conjugated to Alexa Fluor 488 (Life Technologies) (1:100). Cells were mounted on ProLong diamond with 4′,6′-diamidino-2-phenylindole (DAPI) (Invitrogen) and imaged using a Delta-Vision II microscope system with an Olympus IX-71 inverted microscope using a 100× objective. Image processing, analysis, and display were performed using SoftWorx and Adobe Photoshop. Adjustments to brightness and contrast were made for display purposes. For quantification of PfHsp70x-HA fluorescence, PfEMP1 export, and MAHRP1 export, PfHsp70x-*glmS* and PfHsp70x-*M9* parasites were grown in the presence of 7.5 mM GlcN for 72 h, then fixed and stained with anti-HA, anti-ATS, and anti-MAHRP1 as described above. Cells were imaged as described above. The mean fluorescence intensity (MFI) for each protein was calculated as described (9). Briefly, ImageJ was used to calculate the MFI for the whole infected RBC (PfHsp70x) or the infected RBC minus the parasite in order to quantify the exported fraction (PfEMP1and MAHRP1). Differential interference contrast (DIC) images were used to exclude the parasite from analysis when calculating the MFI of the PfEMP1 and MAHRP1 exported fraction. Data were plotted using Prism (GraphPad Software, Inc.).

Human serum staining. 3D7 and PfHsp70x-KO parasites were synchronized to the ring stage by incubating infected RBCs with 5% D-sorbitol (Amresco, Inc.) for 10 min at 37°C. The parasites were washed three times with culture medium and then allowed to proceed through the life cycle to the schizont stage. The cultures were incubated 1:10 with either pooled immune sera from Kenya or nonimmune serum from the United States for 30 min at 37°C with shaking on an orbital shaker at 880 rpm. All study procedures and instruments involving human subjects, data and sample collection, processing, and testing were approved by the University of Georgia and Centers for Disease Control and Prevention Institutional Review Boards and the Kenya Medical Research Institute Ethical Review Board. All participants provided informed, written consent under the auspices of these approved protocols (33). The serum was washed from the parasites three times with culture medium, and goat-anti-human IgG Fc conjugated to phycoerythrin (PE) was added to the parasites (1:500) (Fisher Scientific, 50-112-8944). The secondary antibody was incubated with the parasites for 30 min at 37°C with shaking. The parasites were washed three times with culture medium and resuspended in PBS, fluorescence was measured with a flow cytometer (CytoFLEX; Beckman Coulter), and data were analyzed using FlowJo software (Treestar, Inc.). Immune serum samples were collected as described above, and all samples have been deidentified (33, 44).

SUPPLEMENTAL MATERIAL

Supplemental material for this article may be found at https://doi.org/10.1128/mSphere.00363-17.

FIG S1, TIF file, 2.4 MB.

FIG S2, TIF file, 1.6 MB.

FIG S3, TIF file, 0.2 MB.

ACKNOWLEDGMENTS

REFERENCES

1. World Health Organization. 2016. World malaria report. World Health Organization, Geneva, Switzerland.

2. Cowman AF, Healer J, Marapana D, Marsh K. 2016. Malaria: biology and disease. Cell 167:610–624. https://doi.org/10.1016/j.cell.2016.07.055.

3. Nilsson SK, Childs LM, Buckee C, Marti M. 2015. Targeting human transmission biology for malaria elimination. PLoS Pathog 11:e1004871. https://doi.org/10.1371/journal.ppat.1004871.

4. Desai SA. 2014. Why do malaria parasites increase host erythrocyte permeability? Trends Parasitol 30:151–159. https://doi.org/10.1016/j.pt.2014.01.003.

5. Maier AG, Cooke BM, Cowman AF, Tilley L. 2009. Malaria parasite proteins that remodel the host erythrocyte. Nat Rev Microbiol 7:341–354. https://doi.org/10.1038/nrmicro2110.

6. Marti M, Good RT, Rug M, Knuepfer E, Cowman AF. 2004. Targeting malaria virulence and remodeling proteins to the host erythrocyte. Science 306:1930–1933. https://doi.org/10.1126/science.1102452.

7. Hiller NL, Bhattacharjee S, Van Ooij C, Liolios K, Harrison T, Lopez-Estraño C, Haldar K. 2004. A host-targeting signal in virulence proteins reveals a secretome in malarial infection. Science 306:1934–1937. https://doi.org/10.1126/science.1102737.

8. Klemba M, Goldberg DE. 2005. Characterization of plasmepsin V, a membrane-bound aspartic protease homolog in the endoplasmic reticulum of Plasmodium falciparum. Mol Biochem Parasitol 143:183–191. https://doi.org/10.1016/j.molbiopara.2005.05.015.

9. Russo I, Babbitt S, Muralidharan V, Butler T, Oksman A, Goldberg DE. 2010. Plasmepsin V licenses Plasmodium proteins for export into the host erythrocyte. Nature 463:632–636. https://doi.org/10.1038/nature08726.

10. Haase S, Herrmann S, Grüring C, Heiber A, Jansen PW, Langer C, Treeck M, Cabrera A, Bruns C, Struck NS, Kono M, Engelberg K, Ruch U, Stunnenberg HG, Gilberger TW, Spielmann T. 2009. Sequence requirements for the export of the Plasmodium falciparum Maurer's clefts protein REX2. Mol Microbiol 71:1003–1017. https://doi.org/10.1111/j.1365-2958.2008.06582.x.

11. Grüring C, Heiber A, Kruse F, Flemming S, Franci G, Colombo SF, Fasana E, Schoeler H, Borgese N, Stunnenberg HG, Przyborski JM, Gilberger TW, Spielmann T. 2012. Uncovering common principles in protein export of malaria parasites. Cell Host Microbe 12:717–729. https://doi.org/10.1016/j.chom.2012.09.010.

12. de Koning-Ward TF, Gilson PR, Boddey JA, Rug M, Smith BJ, Papenfuss AT, Sanders PR, Lundie RJ, Maier AG, Cowman AF, Crabb BS. 2009. A newly discovered protein export machine in malaria parasites. Nature 459:945–949. https://doi.org/10.1038/nature08104.

13. Gehde N, Hinrichs C, Montilla I, Charpian S, Lingelbach K, Przyborski JM. 2009. Protein unfolding is an essential requirement for transport across the parasitophorous vacuolar membrane of Plasmodium falciparum. Mol Microbiol 71:613–628. https://doi.org/10.1111/j.1365-2958.2008.06552.x.

14. Riglar DT, Rogers KL, Hanssen E, Turnbull L, Bullen HE, Charnaud SC, Przyborski J, Gilson PR, Whitchurch CB, Crabb BS, Baum J, Cowman AF. 2013. Spatial association with PTEX complexes defines regions for effector export into Plasmodium falciparum-infected erythrocytes. Nat Commun 4:1415. https://doi.org/10.1038/ncomms2449.

15. Sleebs BE, Lopaticki S, Marapana DS, O'Neill MT, Rajasekaran P, Gazdik M, Günther S, Whitehead LW, Lowes KN, Barfod L, Hviid L, Shaw PJ, Hodder AN, Smith BJ, Cowman AF, Boddey JA. 2014. Inhibition of plasmepsin V

16. Hodder AN, Sleebs BE, Czabotar PE, Gazdik M, Xu Y, O'Neill MT, Lopaticki S, Nebl T, Triglia T, Smith BJ, Lowes K, Boddey JA, Cowman AF. 2015. Structural basis for plasmepsin V inhibition that blocks export of malaria proteins to human erythrocytes. Nat Struct Mol Biol 22:590–596. https://doi.org/10.1038/nsmb.3061.

17. Beck JR, Muralidharan V, Oksman A, Goldberg DE. 2014. PTEX component HSP101 mediates export of diverse malaria effectors into host erythrocytes. Nature 511:592–595. https://doi.org/10.1038/nature13574.

18. Elsworth B, Matthews K, Nie CQ, Kalanon M, Charnaud SC, Sanders PR, Chisholm SA, Counihan NA, Shaw PJ, Pino P, Chan JA, Azevedo MF, Rogerson SJ, Beeson JG, Crabb BS, Gilson PR, de Koning-Ward TF. 2014. PTEX is an essential nexus for protein export in malaria parasites. Nature 511:587–591. https://doi.org/10.1038/nature13555.

19. Maier AG, Rug M, O'Neill MT, Brown M, Chakravorty S, Szestak T, Chesson J, Wu Y, Hughes K, Coppel RL, Newbold C, Beeson JG, Craig A, Crabb BS, Cowman AF. 2008. Exported proteins required for virulence and rigidity of Plasmodium falciparum-infected human erythrocytes. Cell 134:48–61. https://doi.org/10.1016/j.cell.2008.04.051.

20. Külzer S, Charnaud S, Dagan T, Riedel J, Mandal P, Pesce ER, Blatch GL, Crabb BS, Gilson PR, Przyborski JM. 2012. Plasmodium falciparum-encoded exported hsp70/hsp40 chaperone/co-chaperone complexes within the host erythrocyte. Cell Microbiol 14:1784–1795. https://doi.org/10.1111/j.1462-5822.2012.01840.x.

21. Rhiel M, Bittl V, Tribensky A, Charnaud SC, Strecker M, Müller S, Lanzer M, Sanchez C, Schaeffer-Reiss C, Westermann B, Crabb BS, Gilson PR, Külzer S, Przyborski JM. 2016. Trafficking of the exported P. falciparum chaperone PfHsp70x. Sci Rep 6:36174. https://doi.org/10.1038/srep36174.

22. Mesén-Ramírez P, Reinsch F, Blancke Soares A, Bergmann B, Ullrich AK, Tenzer S, Spielmann T. 2016. Stable translocation intermediates jam global protein export in Plasmodium falciparum parasites and link the PTEX component EXP2 with translocation activity. PLoS Pathog 12:e1005618. https://doi.org/10.1371/journal.ppat.1005618.

23. Elsworth B, Sanders PR, Nebl T, Batinovic S, Kalanon M, Nie CQ, Charnaud SC, Bullen HE, de Koning Ward TF, Tilley L, Crabb BS, Gilson PR. 2016. Proteomic analysis reveals novel proteins associated with the Plasmodium protein exporter PTEX and a loss of complex stability upon truncation of the core PTEX component, PTEX150. Cell Microbiol 18:1551–1569. https://doi.org/10.1111/cmi.12596.

24. Muralidharan V, Oksman A, Pal P, Lindquist S, Goldberg DE. 2012. Plasmodium falciparum heat shock protein 110 stabilizes the asparagine repeat-rich parasite proteome during malarial fevers. Nat Commun 3:1310. https://doi.org/10.1038/ncomms2306.

25. Prommana P, Uthaipibull C, Wongsombat C, Kamchonwongpaisan S, Yuthavong Y, Knuepfer E, Holder AA, Shaw PJ. 2013. Inducible knockdown of Plasmodium gene expression using the glmS ribozyme. PLoS One 8:e73783. https://doi.org/10.1371/journal.pone.0073783.

26. Muralidharan V, Oksman A, Iwamoto M, Wandless TJ, Goldberg DE. 2011. Asparagine repeat function in a Plasmodium falciparum protein assessed via a regulatable fluorescent affinity tag. Proc Natl Acad Sci U S A 108:4411–4416. https://doi.org/10.1073/pnas.1018449108.

27. Pei Y, Miller JL, Lindner SE, Vaughan AM, Torii M, Kappe SHI. 2013.

Plasmodium yoelii inhibitor of cysteine proteases is exported to exomembrane structures and interacts with yoelipain-2 during asexual blood-stage development. Cell Microbiol 15:1508–1526. https://doi.org/10.1111/cmi.12124.

28. Nacer A, Claes A, Roberts A, Scheidig-Benatar C, Sakamoto H, Ghorbal M, Lopez-Rubio JJ, Mattei D. 2015. Discovery of a novel and conserved Plasmodium falciparum exported protein that is important for adhesion of PfEMP1 at the surface of infected erythrocytes. Cell Microbiol 17:1205–1216. https://doi.org/10.1111/cmi.12430.

29. Ghorbal M, Gorman M, Macpherson CR, Martins RM, Scherf A, Lopez-Rubio JJ. 2014. Genome editing in the human malaria parasite Plasmodium falciparum using the CRISPR-Cas9 system. Nat Biotechnol 32:819–821. https://doi.org/10.1038/nbt.2925.

30. Kats LM, Fernandez KM, Glenister FK, Herrmann S, Buckingham DW, Siddiqui G, Sharma L, Bamert R, Lucet I, Guillotte M, Mercereau-Puijalon O, Cooke BM. 2014. An exported kinase (FIKK4.2) that mediates virulence-associated changes in Plasmodium falciparum-infected red blood cells. Int J Parasitol 44:319–328. https://doi.org/10.1016/j.ijpara.2014.01.003.

31. Watermeyer JM, Hale VL, Hackett F, Clare DK, Cutts EE, Vakonakis I, Fleck RA, Blackman MJ, Saibil HR. 2016. A spiral scaffold underlies cytoadherent knobs in Plasmodium falciparum-infected erythrocytes. Blood 127:343–351. https://doi.org/10.1182/blood-2015-10-674002.

32. Spycher C, Rug M, Pachlatko E, Hanssen E, Ferguson D, Cowman AF, Tilley L, Beck HP. 2008. The Maurer's cleft protein MAHRP1 is essential for trafficking of PfEMP1 to the surface of Plasmodium falciparum-infected erythrocytes. Mol Microbiol 68:1300–1314. https://doi.org/10.1111/j.1365-2958.2008.06235.x.

33. Perrault SD, Hajek J, Zhong K, Owino SO, Sichangi M, Smith G, Shi YP, Moore JM, Kain KC. 2009. Human immunodeficiency virus co-infection increased placental parasite density and transplacental malaria transmission in western Kenya. Am J Trop Med Hyg 80:119–125.

34. Charnaud SC, Dixon MWA, Nie CQ, Chappell L, Sanders PR, Nebl T, Hanssen E, Berriman M, Chan JA, Blanch AJ, Beeson JG, Rayner JC, Przyborski JM, Tilley L, Crabb BS, Gilson PR. 2017. The exported chaperone Hsp70-x supports virulence functions for Plasmodium falciparum blood stage parasites. PLoS One 12:e0181656. https://doi.org/10.1371/journal.pone.0181656.

35. Pasini EME, Kirkegaard M, Mortensen P, Lutz HU, Thomas AW, Mann M. 2006. In-depth analysis of the membrane and cytosolic proteome of red blood cells. Blood 108:791–801. https://doi.org/10.1182/blood-2005-11-007799.

36. Banumathy G, Singh V, Tatu U. 2002. Host chaperones are recruited in membrane-bound complexes by Plasmodium falciparum. J Biol Chem 277:3902–3912. https://doi.org/10.1074/jbc.M110513200.

37. Batinovic S, McHugh E, Chisholm SA, Matthews K, Liu B, Dumont L, Charnaud SC, Schneider MP, Gilson PR, de Koning-Ward TF, Dixon MWA, Tilley L. 2017. An exported protein-interacting complex involved in the trafficking of virulence determinants in Plasmodium-infected erythrocytes. Nat Commun 8:16044. https://doi.org/10.1038/ncomms16044.

38. Egan ES, Jiang RHY, Moechtar MA, Barteneva NS, Weekes MP, Nobre LV, Gygi SP, Paulo JA, Frantzreb C, Tani Y, Takahashi J, Watanabe S, Goldberg J, Paul AS, Brugnara C, Root DE, Wiegand RC, Doench JG, Duraisingh MT. 2015. A forward genetic screen identifies erythrocyte CD55 as essential for Plasmodium falciparum invasion. Science 348:711–714. https://doi.org/10.1126/science.aaa3526.

39. Drew ME, Banerjee R, Uffman EW, Gilbertson S, Rosenthal PJ, Goldberg DE. 2008. Plasmodium food vacuole plasmepsins are activated by falcipains. J Biol Chem 283:12870–12876. https://doi.org/10.1074/jbc.M708949200.

40. Russo I, Oksman A, Goldberg DE. 2009. Fatty acid acylation regulates trafficking of the unusual Plasmodium falciparum calpain to the nucleolus. Mol Microbiol 72:229–245. https://doi.org/10.1111/j.1365-2958.2009.06639.x.

41. Liu J, Gluzman IY, Drew ME, Goldberg DE. 2005. The role of Plasmodium falciparum food vacuole plasmepsins. J Biol Chem 280:1432–1437. https://doi.org/10.1074/jbc.M409740200.

42. Ganesan SM, Morrisey JM, Ke H, Painter HJ, Laroiya K, Phillips MA, Rathod PK, Mather MW, Vaidya AB. 2011. Yeast dihydroorotate dehydrogenase as a new selectable marker for Plasmodium falciparum transfection. Mol Biochem Parasitol 177:29–34. https://doi.org/10.1016/j.molbiopara.2011.01.004.

43. Klemba M, Gluzman I, Goldberg DE. 2004. A Plasmodium falciparum dipeptidyl aminopeptidase I participates in vacuolar hemoglobin degradation. J Biol Chem 279:43000–43007. https://doi.org/10.1074/jbc.M408123200.

44. Avery JW, Smith GM, Owino SO, Sarr D, Nagy T, Mwalimu S, Matthias J, Kelly LF, Poovassery JS, Middii JD, Abramowsky C, Moore JM. 2012. Maternal malaria induces a procoagulant and antifibrinolytic state that is embryotoxic but responsive to anticoagulant therapy. PLoS One 7:e31090. https://doi.org/10.1371/journal.pone.0031090.

45. Boddey JA, Hodder AN, Günther S, Gilson PR, Patsiouras H, Kapp EA, Pearce JA, de Koning-Ward TF, Simpson RJ, Crabb BS, Cowman AF. 2010. An aspartyl protease directs malaria effector proteins to the host cell. Nature 463:627–631. https://doi.org/10.1038/nature08728.